2020 59th IEEE Conference on Decision and Control (CDC)
Jeju Island, Republic of Korea, December 14-18, 2020

Hybrid-MEM-Element Feedforward: With Application to Hysteretic Piezoelectric Actuators

Nard Strijbosch and Tom Oomen

***Abstract*— Hysteresis phenomena can significantly deteriorate the performance when performing servo tasks with piezoelectric actuators. The aim of this paper is to model this nonlinear hysteresis effect using a memory element, in particular a MEM-element, and exploit this model to develop a feedforward controller. A one-to-one mapping is established, leading to both a systematic data-driven learning approach of a hybrid-MEM-element capturing the hysteresis phenomena and a unique inverse allowing for an intuitive design of the feedforward controller. The developed approach is experimentally validated on a piezoelectric actuator, revealing a significant performance improvement.**

I. Introduction

Feedforward can effectively reject known disturbances, e.g., a reference trajectory before these affect the system. A general approach for this type of systems is to determine an inverse model and determine the corresponding parameters [1], [2]. For instance, in linear mechanical systems, Newtons law $F = ma$ can be used, the parameter m can easily be determined using a manual tuning approach, see e.g., [3] for tuning guidelines, and [4] for an automated tuning algorithm.

Feedforward is also effectively applied to compensate for nonlinear friction effects such as Coulomb friction [5]. Coulomb friction leads to nonlinear input-output behaviour. Interestingly, its inverse model can be uniquely determined. By parameterising the feedforward linear in the parameters, it can be very efficiently tuned in a user-friendly manner [3].

Hysteresis phenomena can significantly deteriorate the tracking performance, e.g., in the case of piezoelectric actuators [6], [7], [8]. A wide variety of models have been developed to model the hysteresis effect, including the Ramberg-Osgood model [9], [10], the Maxwell-Slip model [11], the Duhem model [12], the Preisach model [13], and the Prandtl–Ishlinskii model [14].

A key challenge to determine a feedforward controller to compensate for the hysteresis phenomena is non-uniqueness. Due to the history dependency of the hysteresis effect inverting this non-unique input-output mapping is non-trivial. Despite this for some hysteresis models an inverse feedforward exists, see, e.g., [15], [16]. Another solution is to approximate the hysteresis by linear dynamics which can be inverted using existing linear system inversion techniques [17]. Besides this, the inverse multiplicative scheme can be exploited leading to a feedforward controller that does not require an inverse [18]. All these approaches require intensive, possibly nonlinear, identification procedures of the model describing the hysteresis, before determining the feedforward controller.

Although many results have been obtained to model and compensate hysteresis, at present these two stages of modelling and compensating are largely separated. The aim of this paper is to determine a feedforward controller based on the unique inverse of a hybrid-MEM-element merely requiring an identification procedure reminiscent of a polynomial fit.

This leads to the following sub-contributions of this paper:

- C1 A hybrid-MEM-element is proposed to model Ramberg-Osgood-type hysteresis. (Section III)
- C2 A feedforward controller to compensate the hysteresis phenomena is determined which exploits the one-to-one mapping of the hybrid-MEM-element. (Section IV)
- C3 A data-driven learning procedure is introduced to determine the required one-to-one mapping of the feedforward controller (Section V)
- C4 The developed approach is successfully applied to a piezoelectric actuator to compensate for the hysteresis phenomena. (Section VI)

Proofs will be published elsewhere.

II. Problem Formulation

In this section, the key challenge in determining a feedforward controller to compensate hysteresis phenomena is discussed. First, the traditional feedforward approach for linear time-invariant (LTI) systems is discussed. Next, the Ramberg-Osgood model, which is capable of capturing the hysteresis effect in piezoelectric actuators, is introduced. Finally, the problem addressed in this paper is formulated.

A. Feedforward for Servo Control

The main goal in servo control is performing servo tasks, i.e., let an output y of a system G follow a prespecified desired trajectory y_d. A typical control architecture [3] to achieve this is depicted in Fig. 1, where K is the feedback controller and F is the feedforward controller. In the case where all systems are linear time-invariant (LTI) systems, the error e can be expressed as

$$e = S\underbrace{(1 - GF)}_{\text{feedforward}} y_d - \underbrace{S}_{\text{feedback}} v - \underbrace{S}_{\text{feedback}} \eta \qquad (1)$$

where $S = (1+GK)^{-1}$, v a disturbance affecting the system and η a measurement noise. The goal of feedforward is to obtain an input signal u_{ff} for the plant G such that it exactly follows the known reference signal y_d. This is achieved if the

Nard Strijbosch and Tom Oomen are with the Control Systems Technology Group, Departement of Mechanical Engineering, Eindhoven University of Technology, P.O. Box 513, 5600 MB Eindhoven, The Netherlands, e-mail: n.w.a.strijbosch@tue.nl, t.a.e.oomen@tue.nl. This work is part of the research programme VIDI with project number 15698, which is (partly) financed by the Netherlands Organisation for Scientific Research (NWO).

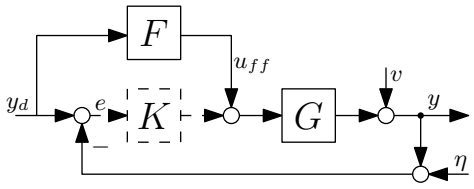

Fig. 1. Control architecture to perform servo tasks.

feedforward controller F is an exact inverse of the system G. The goal of the feedback controller is attenuating the disturbance v, and dealing with uncertainty caused by the residual of $(1 - GF)y_d$ due to incomplete knowledge of G in the design of the feedforward controller F.

For mechanical systems typical feedforward components are; mass feedforward, $F = K_{fa}\frac{\mathrm{d}^2 y_d(t)}{\mathrm{d}t^2}$, viscous friction feedforward, $F = K_{fv}\frac{\mathrm{d}y_d(t)}{\mathrm{d}t}$, and or Coulomb friction $F = K_{fc}\mathrm{sign}\left(\frac{\mathrm{d}y_d(t)}{\mathrm{d}t}\right)$ [3]. For each of these effects only a single parameter needs to be determined, i.e., determine the correct K_{fa}, K_{fd}, and K_{fc}.

In the remainder of this paper the feedback controller K is not taken into account, i.e., $K = 0$.

B. Hysteresis

Hysteresis phenomena in control systems, e.g., when using a piezoelectric actuator, can have a significant impact on control performance [17]. One of the models available in literature that captures hysteresis effects in piezoelectric actuators is the Ramberg-Osgood model [9], [10].

This model is given by an initial skeleton curve

$$\frac{y_h}{y_h^*} = \frac{u_h}{u_h^*}\left(1 + \alpha\left|\frac{u_h}{u_h^*}\right|^{\gamma-1}\right), \tag{2}$$

where y_h is the displacement and u_h is the input signal. The material properties are characterized by the parameters $y_h^*, u_h^* \in \mathbb{R}_{>0}$, $\alpha \in \mathbb{R}_{\geq 0}$, and $\gamma \in \mathbb{R}_{\geq 1}$. This skeleton curve is depicted by the dashed black line (- -) in Fig. 3. After the first direction change of the input signal, referred to as a branching point, the hysteretic behavior is described by

$$\frac{y_h - y_h^{[i]}}{2y_h^*} = \frac{u_h - u_h^{[i]}}{2u_h^*}\left(1 + \alpha\left|\frac{u_h - u_h^{[i]}}{2u_h^*}\right|^{\gamma-1}\right) \tag{3}$$

where the point $(y_h^{[i]}, u_h^{[i]}), i \in \mathbb{N}$ is the most recent point at which the direction of the input has been reversed. Each point $(y_h^{[i]}, u_h^{[i]}), i \in \mathbb{N}$ will be referred to as a branching point. Since, the input signal, u_h, is known, the time instance of the braching points are exactly known.

Example 1 When applying the input signal given by

$$u_h(t) = \begin{cases} 250\sin(2\pi t) & \text{if } t \leq \frac{7}{4}, \\ 125\sin(2\pi t) - 125 & \text{if } t > \frac{7}{4}, \end{cases} \tag{4}$$

see Fig. 2, to the hysteresis model described by (2) and (3) with material characteristics $y_h^* = 1.225{\cdot}10^{-6}$ [m], $u_h^* = 500$ [V], $\gamma = 2$, and $\alpha = 8.0 \cdot 10^{-9}$, leads to the displacement depicted in Fig. 2. The corresponding hysteresis loop to this behaviour is depicted in Fig. 3.

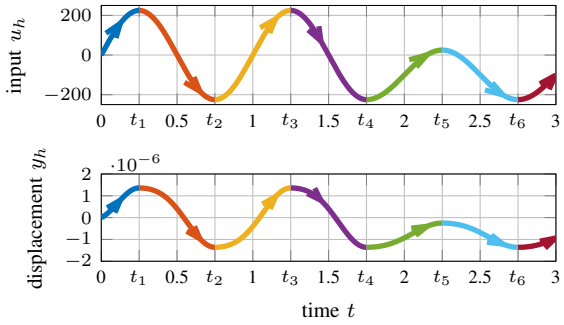

Fig. 2. Input $u_h(t)$ given by (4) and corresponding output $y_h(t)$. Each color indicates one branch of the the hysteresis loop. The time-instance of each branching point is indicated by t_i

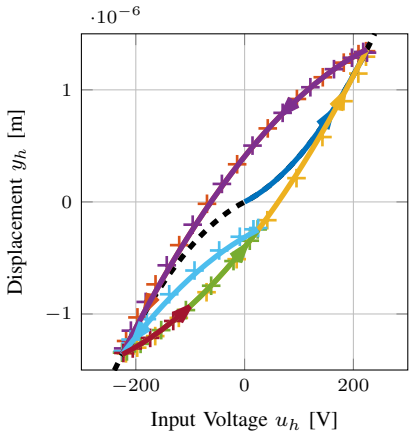

Fig. 3. Hysteresis loop when applying input signal (4). Each color indicates one branch of the the hysteresis loop. The skeleton corresponding to this hysteric behaviour is given by the dashed black line (- -). Experimental data from a piezoelectric actuator is given by crosses (+).

From Fig. 3 it is clear that the mapping from input u_h to output y_h is not one-to-one. Hence, computing the inverse is not straightforward.

C. Problem Formulation

An inverse of this nonlinear behaviour is necessary to compensate the hysteretic effect using a feedforward controller.

This leads to the problem addressed in this paper: developing a feedforward controller to compensate hysteresis without an extensive identification procedure of the hysteresis model. This is achieved through Contributions C1 - C4.

III. Memory Elements

In this section, a hybrid memory (MEM)-element is introduced. Next, it is shown how this hybrid-MEM-element captures the hysteretic behaviour described by (3) leading to Contribution C1 of this paper.

A. Description of memory-element

In this paper, the following structure of a general memory (MEM)-element is considered

$$y(t) = M(p(t))u(t) \tag{5}$$

where $u(t)$ and $y(t)$ are the input and output signals, respectively. The function $M : \mathbb{R} \to \mathbb{R}$ is a one-to-one mapping

TABLE I

INPUT AND OUTPUT SIGNALS FOR THE GENERAL MEM-ELEMENT (5) TO RECOVER WELL KNOWN MEM-ELEMENTS [20]. THE CURRENT AND VOLTAGE ARE DENOTED BY I AND V, RESPECTIVELY.

Element	Input u	Output y
MEMristor	I	V
MEMcapacitor	$\int_0^t I(\tau)\,\mathrm{d}\tau$	V
MEMinductor	$\int_0^t V(\tau)\,\mathrm{d}\tau$	I

which is a function of

$$p(t) = p(t_i) + \int_{t_i}^{t} g(u(\tau))\,\mathrm{d}\tau, \forall t \in [t_i, t_{i+1}) \tag{6}$$

where $g : \mathbb{R} \to \mathbb{R}$. The signal $p(t)$ represents the memory of the input, which can be interpreted as momentum. Following the hybrid system MEM-element definition introduced in [19], the momentum $p(t)$ can be reset at a time instant t_i to a value depending on $p(t_i)$ and $u(t_i)$, i.e., $p(t_i) = f(p(t_i^-), u(t_i^-))$. The time instances of the resets, $t_i, i \in \mathbb{N}$, can depend on the state and input of the system. This allows to model a reset of the memory when the direction of the input changes, i.e., at a branching point.

Disregarding the reset of $p(t)$ and taking $g(u) = u$ all the MEM-elements introduced in [20] can be recovered depending on the choice of the input $u(t)$ and $y(t)$ of the general MEM-element. This is exemplified for the MEMristor in the example below, for other MEM-elements see Table I.

Example 2 A charge controlled MEMristor is given by

$$V(t) = R(q(t))I(t) \tag{7}$$

with V the voltage, I the current and the resistance R depends on the charge $q(t) = \int_0^t I(\tau)\,\mathrm{d}\tau$. This MEMristor can be captured by the general MEM-element (5) by choosing input $u = I$, output $y = V$. Moreover, $M(p) = R(p)$ with the momentum of the MEM-element given by the charge, i.e., $p = q$, which can be achieved with $g(u) = u$, and disregarding the resets.

Besides the electrical MEM-elements as introduced in [20], also mechanical memory elements can be captured by (5). Consider, e.g., the MEMdamper [21] below.

Example 3 A MEMdamper is given by

$$v(t) = \phi(P(t))F(t) \tag{8}$$

with $v(t)$ the velocity, $F(t)$ the applied force, the damping constant ϕ depends on the momentum $P(t) = \int_0^t F(\tau)\,\mathrm{d}\tau$. This MEMdamper can be captured by the general MEM-element (5) by choosing input $u = F$, output $y = v$. Moreover, $M(p) = \phi(p)$ with the momentum of the MEM-element, p, given by the momentum of the damper, P, i.e., $p = P$, which can be achieved with $g(u) = u$, and disregarding the resets.

B. Modelling Hysteresis as MEM-element

One of the key properties of the hysteresis loop of MEM-elements is the zero crossing behaviour, i.e., for each $t \in \mathbb{R}_{>0}$ where the applied input $u(t) = 0$, the corresponding output $y(t) = 0$. This property is evident for the general MEM-element (5), since for any $t \in \mathbb{R}_{>0}$ where $u(t) = 0$ the output $y(t) = 0$, independent of the value of $M(p(t))$. From Fig. 3, it is observed that the hysteresis behaviour in a piezoelectric actuator is not zero-crossing, and can therefore not directly be modelled as a MEM-element of the form (5).

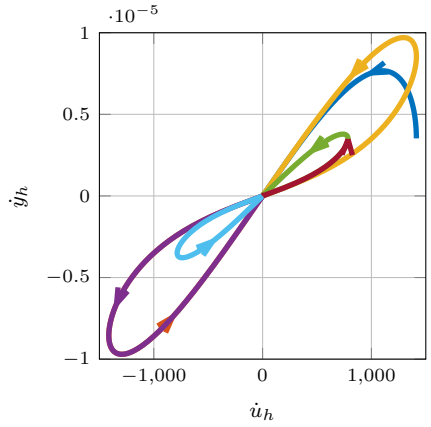

Fig. 4. Hysteresis loop when applying input signal (4).

Interestingly, the relation between the time derivatives of the input $u_h(t)$ and displacement $y_h(t)$ is a zero-crossing relation, as is observed in Fig. 4 and as derived from (3),

$$\dot{y}_h = \frac{y_h^*}{u_h^*}\left(1 + \frac{\alpha\gamma}{(2u_h^*)^{\gamma-1}}\left|u_h - u_h^{[i]}\right|^{\gamma-1}\right)\dot{u}_h. \tag{9}$$

Note that this relation is defined for all $t \in \mathbb{R}_{\geq 0}$ except the branching points t_i, $i \in \mathbb{N}$ since $|u_h(t_i) - u_h^{[i]}| = 0$.

Next, (9) is modelled using the hybrid-MEM-element (5), leading to Contribution C1.

Theorem 4 *Given the hysteresis model* (3) *after its first branching point* $(y_h^{[1]}, u_h^{[1]})$ *given by* (3) *with input* $u_h(t)$*, output* $y_h(t)$ *and parameters* y_h^**,* u_h^**,* α *and* γ*. Then the input-output behaviour from the time-derivative of the input,* $\dot{u}_h(t)$*, to the time-derivative of the output,* $\dot{y}_h(t)$ *is equivalent to the hybrid-MEM-element* (5) *with* $u = \dot{u}_h$*,* $y = \dot{y}_h$*,* $p(t) = |u_h - u_h^{[i]}|$*, and*

$$M(p) = c_1(1 + c_2 p^{c_3}) \tag{10}$$

with $c_1 = \frac{y_h^*}{u_h^*}, \in \mathbb{R}_{>0}$*,* $c_2 = \frac{\alpha\gamma}{(2u_h^*)^{\gamma-1}} \in \mathbb{R}_{\geq 0}$*, and* $c_3 = \gamma - 1 \in \mathbb{R}_{\geq 0}$*. In addition, the momentum* $p(t)$ *can be computed by integration of the absolute value of the input* u *as*

$$p(t) = p(t_i) + \int_{t_i}^{t} |u(\tau)|\,\mathrm{d}\tau = p(t_i) + \int_{t_i}^{t} |\dot{u}_h(\tau)|\,\mathrm{d}\tau \tag{11}$$

where the momentum resets to zero at each branching point, i.e., $p(t_i) = 0$*, where* t_i *corresponds to the* i^{th} *branching point.*

Remark 5 The result of Theorem 4 can be interpreted as follows. The gradient of the hysteresis loop is given by

$$\frac{\dot{y}_h}{\dot{u}_h} = \frac{\partial y_h}{\partial u_h} = M(|u_h - u_h^{[i]}|) = M(p) \tag{12}$$

with M a one-to-one mapping on the interval $[0, \infty)$. Hence, the gradient of the hysteresis loop uniquely depends on

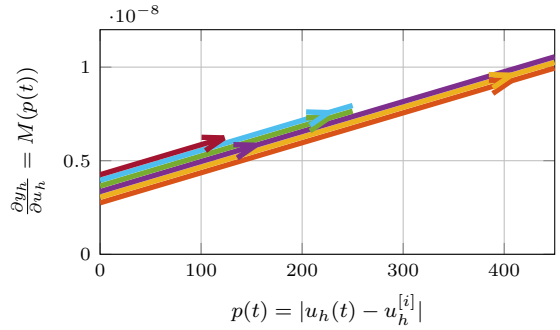

Fig. 5. The gradient $\frac{\partial y_h}{\partial u_h} = M(p(t))$ with respect to $p(t) = |u_h - u_h^{[i]}|$. To visualize the start and end point of each line all lines have a slight offset with respect to each other, in reality all lines perfectly overlap.

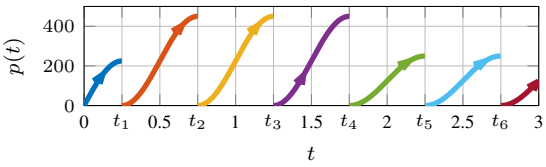

Fig. 6. Momentum signal $p(t)$ corresponding to the input $u_h(t)$ given by (4). Each color indicates one branch of the the hysteresis loop. The time instance of each branching point is indicated by t_i

$p(t) = |u_h(t) - u_h^{[i]}|$. Moreover, at every branching point the value of $u_h^{[i]}$ is reset to u_h, i.e., at each branching point t_i, $p(t_i) = |u_h(t_i) - u_h^{[i]}| = 0$. For the input signal (4) this leads to the momentum trajectory as depicted in Fig. 6.

Because each branching point is known, since it only depends on the applied input, and the unique mapping between the gradient $\frac{\partial y_h}{\partial u_h}$ and $|u_h - u_h^{[i]}|$ an exact inverse can be computed allowing for a feedforward controller to compensate the hysteresis effect in a piezoelectric actuator.

IV. Feedforward for Hysteresis

In this section, a feedforward controller is developed for the hybrid-MEM-element (5). Moreover, exploiting this feedforward controller and the result of Theorem 4 a feedforward controller is developed to compensate hysteresis described by (3), leading to Contribution C2.

A. Feedforward Control for MEM-elements

The goal of the feedforward controller is to determine a control input for a system u_{ff} such that the corresponding output is identical to a desired output trajectory $y_d(t)$, i.e., $y(t) = y_d(t)$, for all $t \in \mathbb{R}_{\geq 0}$. The one-to-one mapping M in the MEM-element (5), enables the unique computation of an input $u_{ff}(t)$ that achieves the desired trajectory $y_d(t)$, leading to the following result.

Theorem 6 *Given a MEM-element of the form* (5) *with input signal* $u(t)$ *and output* $y(t)$*. Moreover, consider the feedforward controller*

$$u_{ff}(t) = M(p_{ff}(t))^{-1} y_d(t) \tag{13}$$

where the momentum $p(t)$ *is the solution of*

$$\dot{p}_{ff}(t) = g\left(M(p_{ff}(t))^{-1} y_d(t)\right) \; \forall t \in [t_i, t_{i+1}) \tag{14}$$

with $p_{ff}(t_1) = p(t_1)$*, and* $p_{ff}(t_i) = f(p_{ff}(t_i^-), u_{ff}(t_i^-))$*, where* t_i, $i \in [2, 3, ...]$ *are the reset instances, and* $p_{ff}(t_i^-) := \lim_{s \uparrow t_i} p_{ff}(s)$, $u_{ff}(t_i^-) := \lim_{s \uparrow t_i} u_{ff}(s)$*. For any desired output trajectory* $y_d(t)$*, the input signal* $u_{ff}(t)$ *generated by* (13)*, applied to the MEM-element* (5)*, leads to an output trajectory satisfying* $y(t) = y_d(t)$ *for all* $t \in \mathbb{R}_{\geq 0}$*.*

Remark 7 Interestingly, when exploiting the result of Theorem 6 for a linear equivalent of a mechanical MEM-element the feedforward controllers as discussed in Section II are recovered. Consider for instance the linear equivalent of the MEMdamper of Example 3, i.e. a linear damper, $v(t) = \Phi F(t)$, with v the velocity, F the force, and $\Phi \in \mathbb{R}_{>0}$ the damping constant. This linear damper can be captured by the general MEM-element (5) by choosing input $u = F$, output $y = v$, and $M = \Phi$. Exploiting Theorem 6 this leads to a feedforward controller given by $F(t) = \frac{1}{\Phi} v_d(t)$ with v_d the desired velocity. This feedforward controller is equivalent to the feedforward controller to compensate viscous friction, $F = K_{fv} \frac{\mathrm{d}y_d(t)}{\mathrm{d}t}$ [3], with $\frac{\mathrm{d}y_d(t)}{\mathrm{d}t} = v_d(t)$ and $\frac{1}{\Phi} = K_{fv}$.

B. Feedforward to compensate hysteresis

Exploiting the results of Theorem 4 a feedforward controller can be derived to compensate the hysteresis that can be described by the Ramberg-Osgood model. This is given by the following result (Contribution C2)

Theorem 8 *Consider a hysteric behaviour after its first branching point given by* (3) *with input* $u_h(t)$*, output* $y_h(t)$ *and parameters* y_h^**,* u_h^**,* α *and* γ*. Moreover, consider the feedforward controller given by*

$$\dot{u}_{hff}(t) = \frac{1}{c_1 + c_2 (p_{hff})^{c_3}} \dot{y}_{hd}(t) \tag{15}$$

where the $\dot{y}_{hd}$ *is the time derivative of the desired trajectory, and* $\dot{u}_{hff}$ *the generated input rate signal and parameters* $c_1 = \frac{y_h^*}{u_h^*}$, $c_2 = \frac{\alpha\gamma}{(2u_h^*)^{\gamma-1}}$, $c_3 = \gamma - 1$ *and the momentum* $p_{hff}(t)$ *is given by*

$$p_{hff}(t) = p_{hff}(t_i) + \int_{t_i}^{t} |\dot{u}_{hff}(\tau)| \, \mathrm{d}\tau \tag{16}$$

with $p_{hff}(t_i) = 0$*, where* t_i *is the time instant of the* i^{th} *branching point. Applying this input rate to the the piezoelectric actuator after its first branching point with* $y_h(0) = y_{hd}(0)$*, and* $u_h(0) = 0$*, leads to the output trajector* $y_h(t) = y_{hd}(t)$ *for all* $t \in \mathbb{R}_{\geq 0}$*.*

From this result, it is concluded that the constants c_1, c_2 and c_3 should be determined.

V. Identification of Feedforward Parameters to Compensate Hysteresis

To determine the correct feedforward for a system with hysteresis, determining the correct constants c_1, c_2 and c_3 is of importance. Next, a systematic method is introduced to determine these parameters, leading to Contribution C3.

The procedure to determine the constants c_1, c_2, and c_3 is based on the fact that the relation

$$M(|u_h - u_h^{[i]}|) = \frac{\dot{y}_h}{\dot{u}_h} = c_1 + c_2 \left| u_h - u_h^{[i]} \right|^{c_3} \tag{17}$$

can be measured during experiments, see, e.g., Fig. 8. Due to the mapping M being one-to-one, the identification problem of the parameters c_1, c_2, c_3 is a nonlinear curve fitting problem. However, in the case c_1 or c_3 is known, the fitting problem can be converted into a convex linear optimization problem. In situation where c_3 is known the unknown parameters c_1, and c_2 clearly appear linear in (17). In the situation where c_1 is known, evaluating (17) subtracted with c_1 on logarithmic scale leads to

$$\log(M(p) - c_1) = \log(c_2 p_3^c) = \underbrace{\log(c_2)}_{c_2'} + c_3 \log(p) \quad (18)$$

with unknown parameters c_2' and c_3 appearing linearly in this equation.

A systematic procedure to determine the parameters from experimental data is introduced below. This procedure iteratively solves these two linear convex optimization problems.

Procedure 1 (Tuning Feedforward for Hysteresis)

1) Perform the following experiment
   - A Apply an input signal, u_h, with multiple direction changes such that the complete range of the piezoelectric actuator is exploited, e.g., a signal (4).
   - B Measure both u_h and y_h.
2) From the measured signals determine or approximate the following signals
   - A $\dot{u}_h$ and $\dot{y}_h$.
   - B Using the signals $\dot{u}_h$ and $\dot{y}_h$ compute $\frac{\partial y_h}{\partial u_h} = \frac{\dot{y}_h}{\dot{u}_h}$.
   - C The signal $|u_h - u_h^{[i]}|$.
3) Identifying the parameters c_1, c_2,and c_3
   - A Determine an initial approximation, $\hat{c}_1$ of the parameter c_1, i.e., the value of $M(0)$.
   - B Evaluate now the data $M(|u_h - u_h^{[i]}|) - c_1)$ with respect to $\log(|u_h - u_h^{[i]}|)$, see, e.g., Fig. 7. If $\hat{c}_1 = c_1$ this relation is linear, see (18). Hence, a linear fitting procedure can be exploited to determine an approximation, $\hat{c}_3$.
   - C Use the value $\hat{c}_3$ to evaluate the relation between $M(|u_h - u_h^{[i]}|)$ and $|u_h - u_h^{[i]}|^{\hat{c}_3}$. If $\hat{c}_3 = c_3$ this relation is linear, see (17). Hence, a linear fitting procedure can be exploited to determine the approximations $\hat{c}_1$ and $\hat{c}_2$.
   - D Perform this procedure iteratively, starting each iteration with the approximation of c_1 that resulted from the previous iteration, until satisfactory results are obtained.

Remark 9 Note that step 3 of Procedure 1 is a curve-fitting problem. Hence, this step can be replaced by any suitable curve-fitting procedure.

VI. Feedforward Applied to a Piezoelectric Actuator

In this section, the developed feedforward controller (15) will be applied to a piezoelectric actuator. First, implementation aspects regarding the parameter identification of the experimental setup and implementation of the feedforward controller are discussed. Next, the developed feedforward approach is applied to the experimental setup and compared to a feedforward approach that disregards the hysteresis effect, leading to Contribution C4.

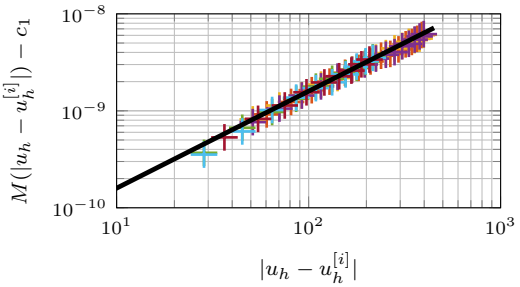

Fig. 7. The mapping $M(|u_h - u_h^{[i]}|) - \hat{c}_1$ on logarithmic scale. Experimental data is given by crosses (+), and its approximation is given by the black line (—). The slope of this relation is used to determine the approximation $\hat{c}_3$, see Step 3.B of Procedure 1.

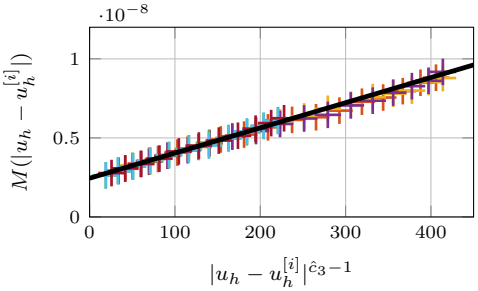

Fig. 8. The mapping $M(|u_h - u_h^{[i]}|)$ on logarithmic scale. Experimental data is given by crosses (+), and its approximation is given by the black line (—). The this linear relation is used to determine the approximations $\hat{c}_1$, and $\hat{c}_2$, see Step 3.C of Procedure 1.

A. Implementation Aspects

Tuning feedforward parameters: Procedure 1 is exploited to determine the parameters c_1, c_2, and c_3 for the piezoelectric actuator considered in this paper. The experimental data as presented in Fig. 7 is exploited to determine the parameter c_3 as described in Step 3.B of Procedure 1. The experimental data as presented in Fig. 8 is epxloited to determine the parameters c_1 and c_2. Due to the small values of both the input rate $\dot{u}_h$ and output velocity $\dot{y}_h$, in Step 2 of Procedure 1, only data points with input rate $\dot{u}_h > 250$ (V/s) are considered to guarantee a sufficiently large signal to noise ratio.

Implementation of feedforward controller: Due to the resets in the feedforward controller (15) ordinary differential equation solvers can not directly be used to compute the feedforward signal $\dot{u}_{hff}$ from (15). However, the time-instants of the desired branching points of the hysteresis loop are exactly known given the desired output trajectory. These time-instances t_i are given by the moments where the direction of the desired position trajectory $\dot{y}_{hd}$ changes. Hence, between the time-instances, t_i and t_{i+1} an ordinary differential equation solver can be exploited to solve the

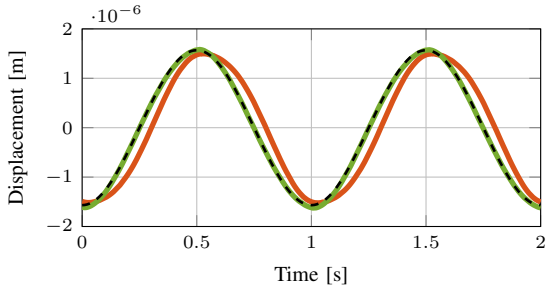

Fig. 9. Experimental results of piezoelectric actuator aiming to follow the reference trajectory (20) (dashed line). The result when applying the feedforward controller developed in Section IV in green (—). The result when neglecting the hysteresis phenomena in red (—).

following smooth nonlinear differential equation

$$\dot{p}_{hff} = |M(p_{hff})^{-1}\dot{y}_{hd}| \tag{19a}$$

$$\dot{u}_{hff} = M(p_{hff})^{-1}\dot{y}_{hd} \tag{19b}$$

with $\dot{p}_{hff}(t_i) = 0$. Solving this set of differential equations results in the input signal u_{hff} which yields the output trajectory $y_h = y_{hd}$.

B. Experimental Results

To validate the performance of the feedforward controller (15) in an experimental environment, the following experiment is performed. The aim of this experiment is to follow a trajectory given by

$$y_{hd} = -1.6 \cdot 10^{-6} \cos(2\pi t) \tag{20}$$

Two feedforward controllers generating a input signal for experimental setup are compared.

1) The developed feedforward controller (15) with parameters identified using Procedure 1.
2) A feedforward controller which approximates the piezoelectric actuator by a linear spring.

The output trajectories measured from the experimental setup for both feedforward controllers are presented in Fig. 9. In Fig. 9 it is observed that the position of the piezoelectric actuator follows the reference when applying the feedforward controller (15). Moreover, a significant performance improvement is observed when applying the developed feedforward compared to the feedforward controller that neglects the hysteresis effect.

VII. Conclusions

In this paper, a feedforward approach to compensate the nonlinear hysteresis effect in piezoelectric actuators is presented, based on hybrid-MEM-elements exploiting a unique inverse which requires only a few parameters that are easy to identify. It is illustrated how the hysteresis effect observed in piezoelectric actuators can be modelled by a hybrid-MEM-element. The one-to-one mapping in the hybrid-MEM-elements is exploited to determine a unique inverse for the nonlinear effect. Moreover, it is illustrated how this one-to-one mapping can be identified for a piezoelectric actuator. Finally, the developed feedforward controller is successfully applied to a piezoelectric actuator.

Acknowledgement

The authors wish to thank Jeroen Setz and Edwin Verschueren for performing the experiments.

References

[1] H. Zhong, L. Pao, and R. de Callafon, "Feedforward control for disturbance rejection: Model matching and other methods," in *2012 24th Chinese Control and Decision Conference (CCDC)*, May 2012, pp. 3528–3533.

[2] J. Butterworth, L. Pao, and D. Abramovitch, "Analysis and comparison of three discrete-time feedforward model-inverse control techniques for nonminimum-phase systems," *Mechatronics*, vol. 22, no. 5, pp. 577 – 587, 2012, special Issue on Distributed Intelligent MEMS: from hardware to software.

[3] T. Oomen, "Control for precision mechatronics," in *Encyclopedia of Systems and Control*, J. Baillieul and T. Samad, Eds. Londen: Springer London, 2019, pp. 1–10.

[4] F. Boeren, T. Oomen, and M. Steinbuch, "Iterative motion feedforward tuning: A data-driven approach based on instrumental variable identification," *Control Engineering Practice*, vol. 37, pp. 11 – 19, 2015.

[5] M. Ruderman and M. Iwasaki, "Observer of nonlinear friction dynamics for motion control," *IEEE Transactions on Industrial Electronics*, vol. 62, no. 9, pp. 5941–5949, 2015.

[6] H. J. M. T. S. Adriaens, W. L. De Koning, and R. Banning, "Modeling piezoelectric actuators," *IEEE/ASME Transactions on Mechatronics*, vol. 5, no. 4, pp. 331–341, Dec 2000.

[7] S. R. Moheimani and A. J. Fleming, *Piezoelectric transducers for vibration control and damping*. Springer Science & Business Media, 2006.

[8] A. J. Fleming and K. K. Leang, *Design, modeling and control of nanopositioning systems*. Springer, 2014.

[9] W. Ramberg and W. R. Osgood, "Description of stress-strain curves by three parameters," 1943.

[10] P. C. Jennings, "Response of simple yielding structures to earthquake excitation," Ph.D. dissertation, California Institute of Technology, 1963.

[11] M. Goldfarb and N. Celanovic, "Modeling piezoelectric stack actuators for control of micromanipulation," *IEEE Control Systems Magazine*, vol. 17, no. 3, pp. 69–79, June 1997.

[12] B. D. Coleman and M. L. Hodgdon, "A constitutive relation for rate-independent hysteresis in ferromagnetically soft materials," *International Journal of Engineering Science*, vol. 24, no. 6, pp. 897 – 919, 1986.

[13] P. Ge and M. Jouaneh, "Modeling hysteresis in piezoceramic actuators," *Precision Engineering*, vol. 17, no. 3, pp. 211 – 221, 1995.

[14] M. Al Janaideh, C.-Y. Su, and S. Rakheja, "Development of the rate-dependent prandtl–ishlinskii model for smart actuators," *Smart Materials and Structures*, vol. 17, no. 3, p. 035026, 2008.

[15] M. Rakotondrabe, C. Clevy, and P. Lutz, "Complete open loop control of hysteretic, creeped, and oscillating piezoelectric cantilevers," *IEEE Transactions on Automation Science and Engineering*, vol. 7, no. 3, pp. 440–450, 2010.

[16] G. Song, Jinqiang Zhao, Xiaoqin Zhou, and J. A. De Abreu-Garcia, "Tracking control of a piezoceramic actuator with hysteresis compensation using inverse preisach model," *IEEE/ASME Transactions on Mechatronics*, vol. 10, no. 2, pp. 198–209, April 2005.

[17] K. K. Leang, Q. Zou, and S. Devasia, "Feedforward control of piezoactuators in atomic force microscope systems," *IEEE Control Systems Magazine*, vol. 29, no. 1, pp. 70–82, Feb 2009.

[18] M. Rakotondrabe, "Bouc-Wen modeling and inverse multiplicative structure to compensate hysteresis nonlinearity in piezoelectric actuators," *IEEE Transactions on Automation Science and Engineering*, vol. 8, no. 2, pp. 428–431, April 2011.

[19] J.-S. Pei, "MEM-spring models combined with hybrid dynamical system approach to represent material behavior," *Journal of Engineering Mechanics*, vol. 144, no. 12, p. 04018109, 2018.

[20] M. Di Ventra, Y. V. Pershin, and L. O. Chua, "Circuit elements with memory: memristors, memcapacitors, and meminductors," *Proceedings of the IEEE*, vol. 97, no. 10, pp. 1717–1724, 2009.

[21] M. E. Fouda, A. G. Radwan, A. S. Elwakil, and N. K. Nawayseh, "Review of the missing mechanical element: Memdamper," in *2015 IEEE International Conference on Electronics, Circuits, and Systems (ICECS)*, 2015, pp. 201–204.